JVI Journals.ASM.org

Hydrophobic and Charged Residues in the Central Segment of the Measles Virus Hemagglutinin Stalk Mediate Transmission of the Fusion-Triggering Signal

Swapna Apte-Sengupta, Chanakha K. Navaratnarajah, Roberto Cattaneo

Department of Molecular Medicine, Mayo Clinic, and Virology and Gene Therapy Track, Mayo Graduate School, Rochester, Minnesota, USA

The pH-independent measles virus membrane fusion process begins when the attachment protein H binds to a receptor. Knowing that the central segment of the tetrameric H stalk transmits the signal to the fusion protein trimer, we investigated how. We document that exact conservation of most residues in the 92 through 99 segment is essential for function. In addition, hydrophobic and charged residues in the 104 through 125 segment, arranged with helical periodicity, are critical for F protein interactions and signal transmission.

Measles virus (MV) is an enveloped negative-strand RNA virus that enters cells by fusing its envelope with the plasma membrane at neutral pH (1, 2). The MV fusion apparatus consists of attachment protein (hemagglutinin, H) tetramers and fusion (F) protein trimers. The type II glycoprotein H is comprised of a 34-residue cytoplasmic tail, a 24-residue transmembrane region, a 95-residue stalk, and a large six-bladed β-propeller head domain that contacts the receptors (3–5) (Fig. 1A). Fusion activation begins upon binding of at least one head in the H tetramer to a receptor (6), which brings about movement of the H head domains (7). The triggering signal is then conducted through the head-proximal dimeric stalk segment (residues 139 through 153) and a flexible tetrameric segment (residues 123 through 138) (4). The next segment (residues 103 through 117) is important for signal transmission to the F trimer (4, 8) (Fig. 1B), a characteristic conserved among *Paramyxoviridae* of different genera (8–10). Moreover, conservation of certain residues within the segment of the MV H stalk comprising residues 92 through 98 is also important for function (11). While the relevance of the central segment of the MV H stalk for signal transmission is clearly established, how it works remains unclear.

Here we analyzed the function of residues 90 through 125 of the MV H stalk by three iterative cycles of mutagenesis. First, since the initial analysis of the influence of Cys substitutions on function covered only residues 103 through 153 (4), we extended it to residue 90. The function of each H protein mutant was assessed by documenting the level of syncytium formation after cotransfection of the corresponding H expression plasmid with the standard F protein expression plasmid (quantitative evaluation of the results as in reference 4). Strikingly, 10 of the 13 new Cys mutants either abolished or strongly reduced fusion (Fig. 1C, positions 90 through 102). The fusion function of these 10 mutants was not rescued after reduction of the disulfide bonds (for methods, see reference 4; data not shown). The three residues that maintained function (93, 96, and 100) had 3-4 periodicity, consistent with helical structure. These results suggest that the segment of the H stalk important for function may extend at least to position 90.

To further characterize the central segment of the H stalk, we subjected it to a more conservative type of mutagenesis. This analysis was based on two small amino acids: alanine to substitute for charged and polar residues and serine to replace apolar residues. The results of the quantitative fusion assays (for methods, see reference 12) are listed at the bottom of Fig. 1C and represented graphically above these values. This analysis revealed the existence of two segments with different characteristics. Five of the 8 residues located in segment 96 through 103 completely lost function after Ser/Ala mutagenesis, whereas mutagenesis of residues 106 and above only rarely resulted in a loss of function. In particular, residues 111, 114, and 118 completely lost function, and residues 115, 121, and 124 partially lost function, revealing 3-4 helical periodicity for this upper segment also.

The third round of mutagenesis focused on those hydrophobic residues that were shown in round 2 to have a significant effect on fusion (group I, L92, F96, I98, I99, V103, L105, F111, L114, I118; 9 residues) and on all the charged residues (group II, K97, D101, E102, R106, R110, D113, K116, D120, K121, K123; 10 residues). Each hydrophobic residue was subjected to conservative and nonconservative mutagenesis (Fig. 2A and B, respectively). The expression, dimerization, and stability of each mutant protein were analyzed by immunoblotting in nonreducing conditions; most mutants had total expression (TEx) values ranging between 40 and 125% of that of standard H, with a few exceptions (Fig. 2A through C, TEx values). Moreover, most mutants had dimer to monomer (D:M) ratios ranging from 1.8 to 6.0, which were thus similar to the 3.7 ratio of standard H (Fig. 2A through C, D:M ratios). These parameters indicate that most mutants were correctly folded and thus stable. As expected, introduction of charges always interfered with function (Fig. 2B). Interestingly, conservative mutations in the 3 most membrane-proximal residues (L92, F96, and I98L) reduced function 2- to 5-fold, whereas the other conservative mutations had minimal effects on function (Fig. 2A).

Mutagenesis of the charged residues revealed a different cluster effect: mutations D113R, K116D, and D120R, which have helical 3-4 periodicity, maintained function, whereas the other 7 oppo-

Received 7 June 2013 **Accepted** 9 July 2013
Published ahead of print 17 July 2013
Address correspondence to Roberto Cattaneo, cattaneo.roberto@mayo.edu.

doi:10.1128/JVI.01547-13

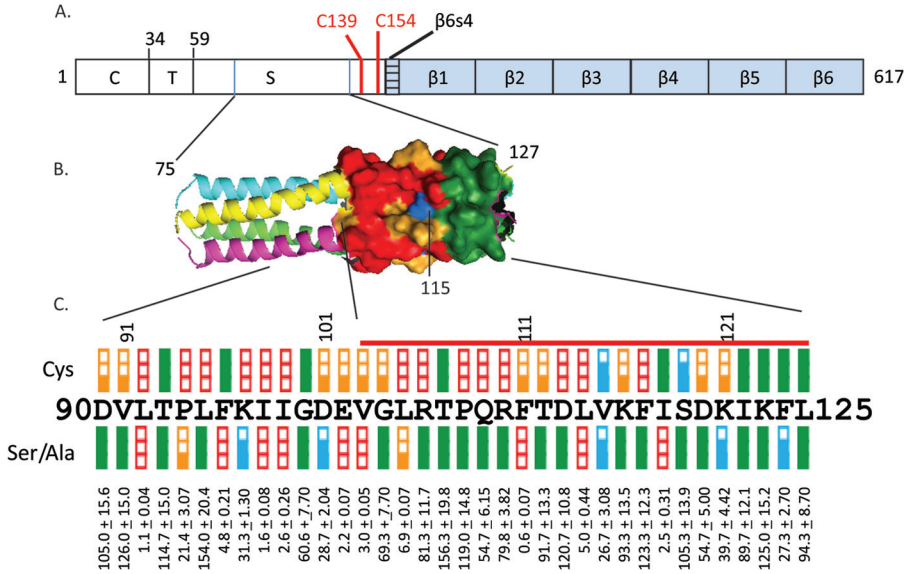

FIG 1 Analysis of the function of the central segment of the MV H stalk. (A) H protein primary structure. From left to right: C, cytoplasmic tail; T, transmembrane region; S, stalk; β1 through -6, head beta-propeller blades 1 through 6. Cys139 and Cys154, involved in intersubunit disulfide bonds, are shown as vertical red lines. (B) Structure-based model of stalk residues 75 through 127 (4). Residues 103 through 125, which were previously analyzed by cysteine mutagenesis (4), are shown in surface representation. The other residues are in backbone representation. Each monomer is shown with a different color: yellow, magenta, green, or blue. Fusion-support function is color coded as follows: green, ≥50%; blue, 26 to 50%; orange, 6 to 25%; red, ≤5%. (C) Fusion-support functions of the H-stalk mutants. (Top row) Fusion scores for all the Cys mutants. Scores for mutants 103 through 125 were previously published (red line) (4); scores for mutants 90 through 102 are new. (Central row) Fusion scores for the Ser or Ala mutants. Fusion-support function is color coded as follows: (top and central rows) filled green box, ≥50%; two-thirds-filled blue box, 26 through 50%; one-third-filled orange box, 6 through 25%; open red box, ≤5%. (Bottom row) Means and standard deviations for three replicates of quantitative fusion assays.

site-charge mutations abolished function (Fig. 2C). Cell surface expression of H mutants was also tested by fluorescence-activated cell sorting, yielding values ranging from 40 to 130% of that of standard H for all mutants (data not shown). Thus, inefficient intracellular transport is unlikely to account for loss of function of the mutants.

We then assessed by coimmunoprecipitation (co-IP) the effect of 16 of the 19 mutations analyzed in the third round of mutagenesis on the interaction of H with F. Mutations D113R, K116D, and D120R were excluded because they had no impact on function. Figure 3A shows a representative co-IP analysis, and Fig. 3B shows the quantification of band intensities of immunoprecipitated H and coimmunoprecipitated F proteins. Figure 3C is a graphic representation of the means and standard deviations of the F to H ratios of all 16 H stalk mutants, calculated based on three independent experiments. The results indicate that the hydrophobic residue L114 and the two charged residues, R110 and K121, are the most important for the interaction with F (F:H ratios of ≤0.1). Additionally, L92, I99, and I118 are also important (F:H ratios of 0.1 to 0.3). Moreover, as expected, introduction of charges in place of hydrophobic residues interfered with the fusion-triggering function (data not shown). Thus, both hydrophobic and charged residues are important for the interaction of H with F as assessed by co-IP. We also note that certain mutations, including F96S, D101R, E102R, F111S, and K123D, modulated fusion while having little or no effect on the formation of the F-H complex as measured by co-IP. These residues may be required for conducting certain conformational changes required for fusion.

In conclusion, we identified a segment of the H stalk of which conservation is essential for function: 5 of 8 Ser/Ala-scanning mutants in the 92 through 99 stalk segment abolished fusion-triggering function. Even conservative mutations in residues 92, 96, and 98 strongly reduced this function, confirming and extending previous observations (11). Specifically, Corey and Iorio showed that conservation of hydrophobicity by substitution with alanine either increased or maintained H and F interactions (11). Here, by replacing two hydrophobic residues with polar residues we reduced the interactions by about half. Together these data indicate that the hydrophobic nature of residues 92 through 99 is important for the interaction with F. However, we do not know whether the reduction in coimmunoprecipitation efficiency is due to direct contacts of the modified side chains with F residues or, perhaps more likely, to indirect effects due to changes in H stalk conformation.

While less sensitive to Ser/Ala scanning, the H stalk segment 104 through 125 is also important for fusion-triggering function, as previously shown by Lee et al. for MV (10) and Ader et al. for canine distemper virus (8). Interestingly, sensitivity to mutation shows 3-4 helical periodicity: mutation of residues 111, 114, and 118 results in complete loss of function. Moreover, mutation of residues 110, 114, and 121 and to a lesser extent 118 interferes with coimmunoprecipitation. In particular, effects on residues 110 and 121 were observed only when mutation was to the opposite charge, but not when mutation was to alanine. Due to 3-4 helical periodicity, these residues, shown in black and gray in Fig. 4A, are vertically aligned on the H stalk model.

Remarkably, we observed that mutation of D113, K116, and D120 to the opposite charge did not interfere with function (Fig. 4B, green residues), while opposite-charge mutants located above or below these positions abolished function (Fig. 4B, red resi-

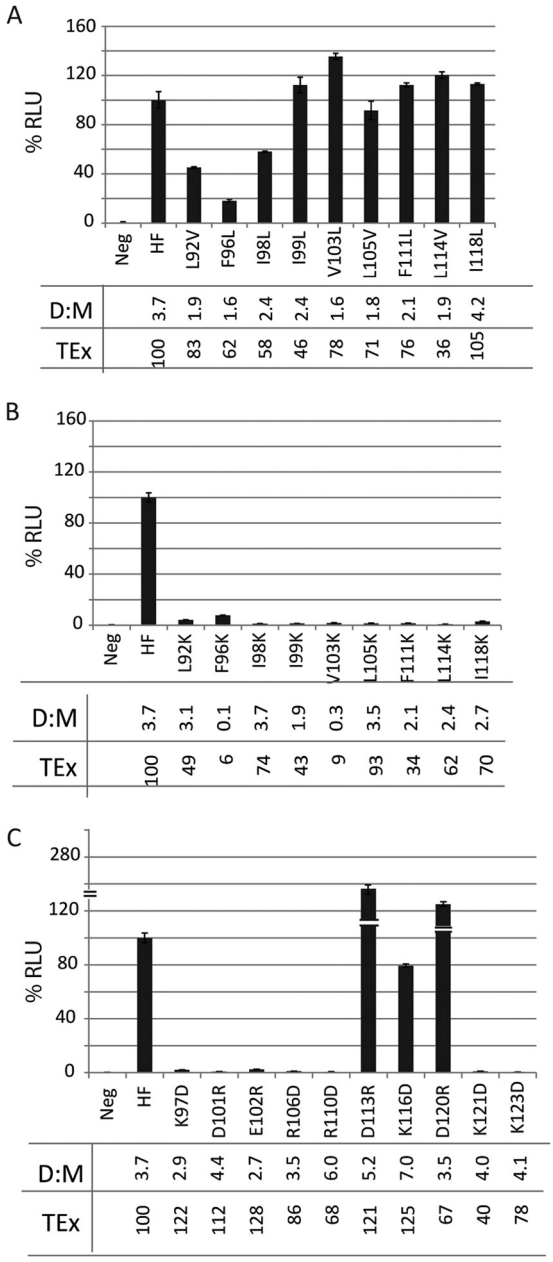

FIG 2 Analysis of the function of the hydrophobic and charged residues based on quantitative fusion assays. (A) Conservative substitution (hydrophobic to hydrophobic); (B) nonconservative substitution (hydrophobic to charge); (C) opposite charge for charged residues. Neg, negative control; HF, positive control. The horizontal axes indicate the identities of the H stalk mutants, and the vertical axes indicate relative luciferase units (RLU). Standard values for H and F (HF) were set at 100%. Means and standard deviations are indicated. Dimer to monomer ratios (D:M) were calculated by separating the cell lysates on a 4 to 15% nonreducing SDS-polyacrylamide gel, blotting to a polyvinylidene difluoride (PVDF) membrane, probing with anti-H_{cyt} antibodies, quantifying the bands using the Typhoon FLA 7000 gel documentation system and ImageQuant 5.0 software, and dividing the intensity of the dimer band by the intensity of the monomer band. Total protein expression (TEx) was calculated by adding the dimer and monomer band intensities. The numbers represent percentiles of expression levels relative to that of standard H.

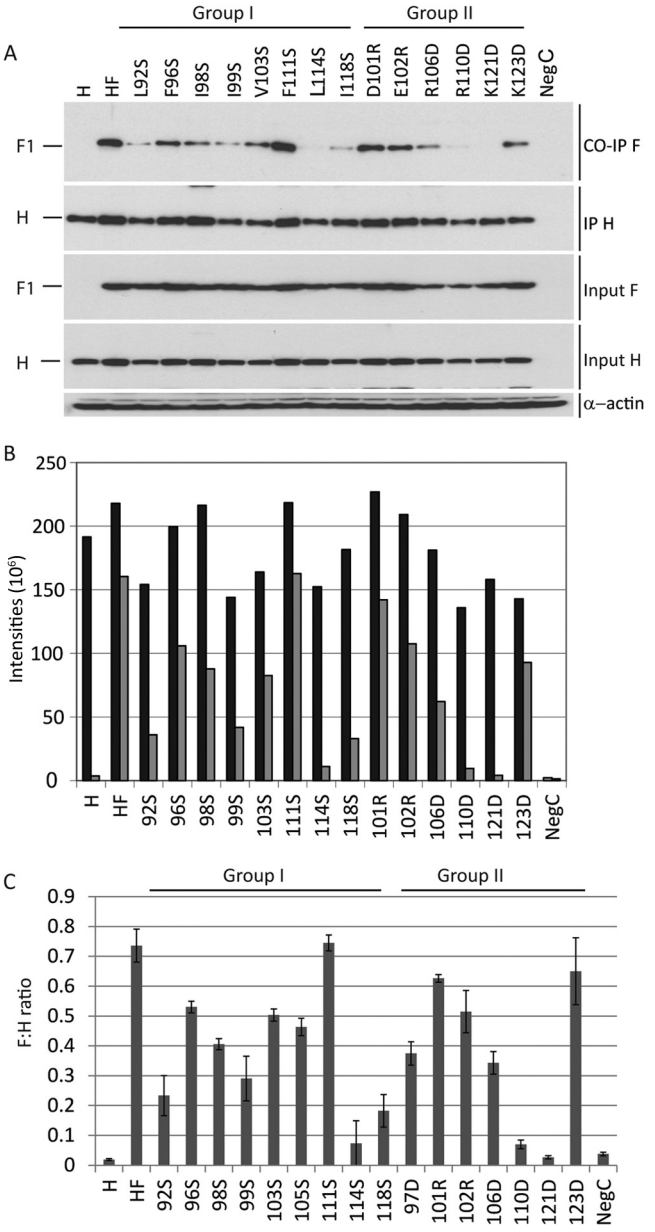

FIG 3 Coimmunoprecipitation analyses of the interactions of the H protein mutants with F. Cells were transfected with the plasmids indicated above the gels or below the columns. (A) Coimmunoprecipitation and total cell lysates. H, H only; HF, standard H and F; next 14 lanes, H mutants cotransfected with standard F protein; NegC, empty plasmid. For immunoprecipitation, the anti-H antibody cl55 (a kind gift from D. Gerlier, INSERM, Lyon, France) was used. Precipitated complexes were separated on a 4 to 15% SDS-polyacrylamide gel, blotted to a PVDF membrane, and probed with anti-F_{cyt} (16) (first and third panels), or anti-H_{cyt} (second and fourth panels) antibodies (16). Positions of F and H proteins are indicated on the left. (B) Quantitative results of the experiment shown in panel A. Black, H-band intensity (after IP); gray, F1 band intensity (after co-IP). The intensities of the bands were quantified using the Typhoon FLA 7000 gel documentation system and ImageQuant 5.0 software; the *y* axes indicate the pixel intensities of the protein bands. For detailed methods, see reference 12. (C) Means and standard deviations of F:H ratios from three experiments. F:H ratios were calculated by dividing the quantities of coimmunoprecipitated F proteins by the quantities of immunoprecipitated H.

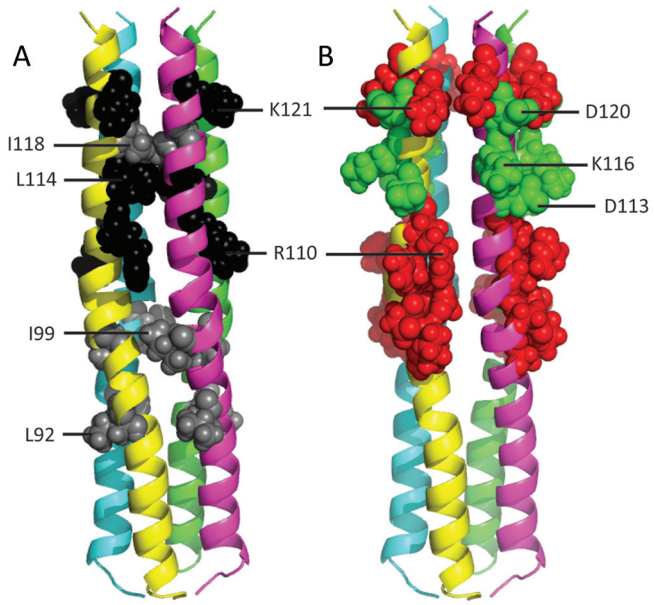

FIG 4 Mutations affecting H:F interactions and effects of introduction of opposite charges on H fusion support function. (A) Mutations affecting H:F interactions. The relevant residues are shown in spherical representation: black shows mutations resulting in F:H ratios of <0.1; gray shows mutations resulting in F:H ratios of 0.1 to 0.3. (B) Effects of introduction of opposite charges on H fusion support function. Charged residues within the 97 through 123 stalk segment are shown in spherical representation. Red shows opposite charge mutations abolishing fusion support function; green shows opposite-charge mutations with no effect on function.

dues). The null effect of opposite charges introduced at residues 113, 116, and 120 indicates that salt bridges do not stabilize the interactions of this segment of the H stalk with F, while salt bridges above or below this segment, as well as hydrophobic interactions, may stabilize H-F complexes.

In combination with the results of extensive Cys mutagenesis of the MV and canine distemper virus stalks (4, 8), our results indicate that mobility of the 104 through 125 stalk segment is essential for function. Interestingly, a recent analysis of the structure of the parainfluenza virus 5 (PIV5) hemagglutinin-neuraminidase (HN) ectodomain reported a "2-heads-up/2-heads-down" conformation (13). In particular, residues 85 through 101 of the PIV5 HN stalk interact with one side of the HN dimer in the heads-down conformation (13). Analogously, one side of the Newcastle disease virus HN dimeric head interacts with the homologous HN stalk (14). Thus, it is conceivable that MV H may also assume 2-heads-down or even 4-heads-down conformations; remarkably, residues 85 through 101 of the PIV5 HN stalk align with residues 108 through 125 of the MV H stalk (4), the segment analyzed here. This implies that certain mutations that cause reductions in H-F coimmunoprecipitation levels may simply reduce the frequency with which an H stalk conformation supporting the interactions with F is available.

In this context, it is interesting to note that MV F and H already hetero-oligomerize in the endoplasmic reticulum (15), whereas F and HN do it only at the cell surface. Thus, while triggering of membrane fusion by H and HN proteins may rely on similar interactions of attachment protein tetramers and F trimers, the temporal sequences of events leading to fusion triggering may differ.

ACKNOWLEDGMENTS

We are grateful to Yusuke Yanagi for Vero/hSLAM cells and Denis Gerlier for the cl55 antibody.

This work was supported by National Institutes of Health grant R01 CA090636 (to R. C.).

REFERENCES

1. **Lamb RA, Parks GD.** 2007. Paramyxovirus: the viruses and their replication, p 1305–1340. *In* Knipe DM, Howley PM, Griffin DE, Lamb RA, Martin MA, Roizman B, Straus SE (ed), Fields virology, 5th ed, vol 1. Lippincott Williams & Wilkins, Philadelphia, PA.
2. **Navaratnarajah CK, Miest TS, Carfi A, Cattaneo R.** 2012. Targeted entry of enveloped viruses: measles and herpes simplex virus I. Curr. Opin. Virol. **2:**43–49.
3. **Hashiguchi T, Kajikawa M, Maita N, Takeda M, Kuroki K, Sasaki K, Kohda D, Yanagi Y, Maenaka K.** 2007. Crystal structure of measles virus hemagglutinin provides insight into effective vaccines. Proc. Natl. Acad. Sci. U. S. A. **104:**19535–19540.
4. **Navaratnarajah CK, Negi S, Braun W, Cattaneo R.** 2012. Membrane fusion triggering: three modules with different structure and function in the upper half of the measles virus attachment protein stalk J. Biol. Chem. **287:**38543–38551.
5. **Mateo M, Navaratnarajah CK, Syed S, Cattaneo R.** 2013. The measles virus hemagglutinin β-propeller head β4-β5 hydrophobic groove governs functional interactions with nectin-4 and CD46 but not with the signaling lymphocytic activation molecule. J. Virol. **87:**9208–9216.
6. **Brindley MA, Takeda M, Plattet P, Plemper RK.** 2012. Triggering the measles virus membrane fusion machinery. Proc. Natl. Acad. Sci. U. S. A. **109:**E3018–E3027.
7. **Navaratnarajah CK, Oezguen N, Rupp L, Kay L, Leonard VHJ, Braun W, Cattaneo R.** 2011. The heads of the measles virus attachment protein move to transmit the fusion-triggering signal. Nat. Struct. Mol. Biol. **18:**128–134.
8. **Ader N, Brindley MA, Avila M, Origgi FC, Langedijk JPM, Örvell C, Vandevelde M, Zurbriggen A, Plemper RK, Plattet P.** 2012. Structural rearrangements of the central region of the morbillivirus attachment protein stalk domain trigger F protein refolding for membrane fusion. J. Biol. Chem. **287:**16324–16334.
9. **Bose S, Welch BD, Kors CA, Yuan P, Jardetzky TS, Lamb RA.** 2011. Structure and mutagenesis of the parainfluenza virus 5 hemagglutinin-neuraminidase stalk domain reveals a four-helix bundle and the role of the stalk in fusion promotion. J. Virol. **85:**12855–12866.
10. **Lee JK, Prussia A, Paal T, White LK, Snyder JP, Plemper RK.** 2008. Functional interaction between paramyxovirus fusion and attachment proteins. J. Biol. Chem. **283:**16561–16572.
11. **Corey EA, Iorio RM.** 2007. Mutations in the stalk of the measles virus hemagglutinin protein decrease fusion but do not interfere with virus-specific interaction with the homologous fusion protein. J. Virol. **81:**9900–9910.
12. **Apte-Sengupta S, Negi S, Leonard VHJ, Oezguen N, Navaratnarajah CK, Braun W, Cattaneo R.** 2012. Base of the measles virus fusion trimer head receives the signal that triggers membrane fusion. J. Biol. Chem. **287:**33026–33035.
13. **Welch BD, Yuan P, Bose S, Kors CA, Lamb RA, Jardetzky TS.** 2013. Structure of the parainfluenza virus 5 (PIV5) hemagglutinin-neuraminidase (HN) ectodomain. PLoS Pathog. **8:**8. doi:10.1371/journal.ppat.1003534.
14. **Yuan P, Swanson KA, Leser GP, Paterson RG, Lamb RA, Jardetzky TS.** 2011. Structure of the Newcastle disease virus hemagglutinin-neuraminidase (HN) ectodomain reveals a four-helix bundle stalk. Proc. Natl. Acad. Sci. U. S. A. **108:**14920–14925.
15. **Plemper RK, Hammond AL, Cattaneo R.** 2001. Measles virus envelope glycoproteins hetero-oligomerize in the endoplasmic reticulum. J. Biol. Chem. **276:**44239–44246.
16. **Cathomen T, Naim HY, Cattaneo R.** 1998. Measles viruses with altered envelope protein cytoplasmic tails gain cell fusion competence. J. Virol. **72:**1224–1234.